Influence of Proline Residues on the Antibacterial and Synergistic Activities of α-Helical Peptides†

Lijuan Zhang,‡ Roland Benz,§ and Robert E. W. Hancock*,‡

Department of Microbiology and Immunology, University of British Columbia, #300-6174 University Boulevard, Vancouver V6T 1Z3, Canada, and Lehrstuhl fur Biotechnologie, Theodor-Boveri-Institut der Universitat, Am Hubland, D-97074 Wurzburg, Germany

Received February 19, 1999; Revised Manuscript Received April 9, 1999

ABSTRACT: To investigate the influence of proline residues on the activity of α-helical peptides, variants were synthesized with insertions of proline residues to create peptides without proline, or with one or two prolines. The influence of the proline-induced bends was assessed by circular dichroism in the presence of liposomes, and the ability of the peptides to kill microorganisms, to permeabilize the outer and cytoplasmic membranes of *Escherichia coli*, to bind to liposomes, to form channels in planar lipid bilayers, and to synergize with conventional antibiotics. Representative peptides adopted α-helical conformations in phosphatidylcholine/phosphatidylglycerol (POPC/POPG, 7:3) liposomes as well as in 60% trifluoroethanol solution, as revealed by circular dichroism (CD) spectroscopy. However, the percent of helicity decreased as the number of proline residues increased. Tryptophan fluorescence spectroscopy showed that all of these peptides inserted into the membranes of liposomes as indicated by a blue shift in the emission maximum and an increase in the fluorescence intensity of the single tryptophan at residue 2. Quenching experiments further prove that the tryptophan residue was no longer accessible to the aqueous quencher KI. The peptide that lacked proline exhibited the highest activity [minimal inhibitory concentrations (MICs) of 0.5−4 μg/mL] against all tested Gram-negative and Gram-positive bacteria, but was hemolytic at 8 μg/mL. The single-proline peptides exhibited intermediate antibacterial activity. Peptides with two proline residues were even less active with moderate MICs only against *E. coli*. With only one exception from each group, the peptides were nonhemolytic. The ability of the peptides to demonstrate synergy in combination with conventional antibiotics increased as the antibacterial effectiveness decreased. All peptides bound to bacterial lipopolysaccharide and permeabilized the outer membrane of *E. coli* to similar extents. However, their ability to permeabilize the cytoplasmic membrane of *E. coli* as assessed by the unmasking of cytoplasmic β-galactosidase decreased substantially as the number of proline residues increased. Correspondingly, increasing the number of proline residues caused a decreased ability to form channels in planar lipid bilayers, and the hemolytic, proline-free peptide tended to cause rapid breakage of planar membranes. Thus, the number of bends created by insertion of proline residues is an important determinant of antimicrobial, hemolytic, and synergistic activity.

Antimicrobial peptides are a key component of innate immunity (*1*). To date, more than 500 different antimicrobial peptides have been isolated from a wide range of animal, plant, and bacterial species. These peptides exhibit a broad spectrum of killing activity in vitro against various targets, including bacteria, fungi, enveloped viruses, parasites, and even tumor cells (*2*, *3*). Thus, they are of special pharmaceutical interest due to the emergence of increasing numbers of medically important antibiotic-resistant bacteria and the lack of new antibiotic classes introduced into the clinic in the past 30 years. Many antimicrobial peptides share two unique features, in that they are polycationic and amphipathic. These characteristics are thought to allow them to interact with the negatively charged surface molecule lipopolysaccharide (LPS)[1] (*4*), and/or to interact with and insert into the negatively charged cytoplasmic membranes of bacteria (*5*). However, the target of these cationic peptides is not well-understood, and the mechanism of action is still a matter of debate. Although formation of voltage-gated and cation-selective ion channels or pores has been evident in planar lipid bilayers for many peptides (*6*, *7*), there has been little convincing evidence to link such interactions to the event(s) causing bacterial cell death.

The naturally occurring peptides are generally from 12 to 50 amino acids long, and most of them fit into four major

† This work was supported by the funding of the Canadian Bacterial Disease Network and Canadian Cystic Fibrosis Foundation's SPARx Program to R.E.W.H. and of the Deutsche Forschungsgemeinschaft (Project B9 of Sonderforschungsbereich 176) and of the Fonds der Chemischen Industrie to R.B.

* To whom correspondence should be addressed. Telephone: (604) 822-2682. Fax: (604) 822-6041. E-mail: bob@cmdr.ubc.ca.

‡ University of British Columbia.

§ Theodor-Boveri-Institut der Universitat.

[1] Abbreviations: NPN, 1-*N*-phenylnaphthylamine; CCCP, carbonyl cyanide-*m*-chlorophenyl hydrazone; ONPG, *o*-nitrophenyl β-D-galactoside; POPC, 1-pamitoyl-2-oleoyl-*sn*-glycero-3-phosphocholine; POPG, 1-palmitoyl-2-oleoyl-*sn*-glycero-3-phosphoglycerol; MIC, minimal inhibitory concentration; LPS, lipopolysaccharide; Nal, nalidixic acid; Cm, chloramphenicol; CD, circular dichroism.

10.1021/bi9904104 CCC: $18.00
Published on Web 05/27/1999

structural groups, namely, α-helices, *β*-sheets, extended helices, and loops (*6*). The α-helical peptides are a large family of linear, amphipathic polypeptides of less than 40 amino acids and are devoid of cysteine residues. These peptides vary considerably in chain length, hydrophobicity, and overall distribution of charges, but fold into a common amphipathic α-helical structure upon association with membranes (*8*). They are short and easy to synthesize by solid-phase synthesis, and thus have been subjected to extensive studies of structure−activity relationships. Studies of synthetic α-helical model peptides differing at one or more sequence positions have revealed important aspects of structure−function relationships. A number of parameters, including overall positive charge, average hydrophobicity, hydrophobic moment, helical propensity, angle subtended by the positively charged residues, etc., have been shown to modulate the activity of α-helical peptides. Increasing the total positive charge often, but not obligatorily, results in enhanced antibacterial activity (*9*, *10*). Enhancement of the hydrophobicity and hydrophobic moment generally leads to both enhanced antibacterial and hemolytic activity (*11*, *12*).

Most of the naturally occurring antibacterial α-helical peptides carry a proline and/or one or two consecutive glycines in their sequences. Due to the presence of these residues, such peptides do not fold into uninterrupted α-helices, but rather form helix−bend−helix structures. Relatively few studies have investigated the importance of prolines in the activity and specificity of antimicrobial peptides. Gazit et al. (*13*) investigated cecropin P1, and found that inclusion of a second proline at the C-terminus decreased antibacterial activity, and reduced the degree of liposomal membrane penetration. In a 16-residue model cationic peptide, Thennarasu and Nagaraj (*14*) found that removing a proline in the central position actually decreased hemolytic activity without decreasing antibacterial activity. Conversely, removal of proline-7 from pardaxin made the molecule more hemolytic (*15*). For cecropin A, insertion of a second proline residue at position 4 or 8 had no effect on activity against *Escherichia coli*, but caused a 3−5-fold decrease in activity against *Pseudomonas aeruginosa*, as did virtually every other substitution in the first eight amino acids (*16*). However, none of these studies investigated the mechanisms underlying these observations, except to show a decrease in peptide α-helicity in organic solvent upon proline insertion.

Recently, we employed a semirandom DNA mutagenesis technique to mutagenize a peptide gene to produce variants of α-helical peptides (*17*). Of the clones selected from a recombinant library, we obtained eight peptides having a limited number of amino acid substitutions and either lacking proline or having one or two proline residues inserted at two different positions, dividing them into three groups, nonbent, single-bend, and double-bend peptides. Here we have studied the influence of these proline insertions on the interaction with bacteria, and show that the induced bends dramatically influenced the antimicrobial activity, cytoplasmic membrane permeabilization, channel forming activity, and ability to act synergistically in combination with conventional antibiotics.

EXPERIMENTAL PROCEDURES

Strains and Reagents. The main bacterial strains used for antimicrobial activity assays included *E. coli* UB1005 (F^-, *nalA37*, *metB1*) (*18*), wild-type strains of *Salmonella typhimurium* 14028s (*19*), *Streptomyces aureus* ATCC25923 (from D. Speert, Department of Medicine, University of British Columbia), *P. aeruginosa* K799 (*20*), and a clinical isolate of *Staphylococcus epidermidis* (from A. Chow, Department of Medicine, University of British Columbia). All the strains were grown in Mueller Hinton (MH) broth (Difco Laboratories, Detroit, MI) at 37 °C unless otherwise indicated. The lipopolysaccharides (LPS) of *E. coli* UB1005 and *P. aeruginosa* H103 used for the dansyl polymyxin B replacement assay were isolated as described by Moore et al. (*21*). *E. coli* UB1005 and *E. coli* ML-35 (*lacI*$^-$, *lacY*$^-$, *lacZ*$^+$) (*22*) were used for outer and cytoplasmic membrane permeability assays, respectively. *E. coli* KF130 (*gyrA*) and KF111 (*gyrA*, *nfxB*) were resistant to nalidixic acid with minimal inhibitory concentrations (MICs) of 312 and 625 μg/mL, respectively, and MICs of 2 and 4 μg/mL for chloramphenicol, respectively (*23*). *P. aeruginosa* H744 was a *nalB* mutiple-antibiotic-resistant efflux mutant with MICs of 312 and 64 μg/mL for nalidixic acid and chloramphenicol, respectively (*24*). *P. aeruginosa* H374 was an *nfxB* efflux mutant with MICs of 2500 μg/mL for nalidixic acid and 8 μg/mL for chloramphenicol (*25*).

Chloramphenical, nalidixic acid, polymyxin B, 1-*N*-phenylnaphthylamine (NPN), carbonyl cyanide-*m*-chlorophenyl hydrazone, and *o*-nitrophenyl *β*-D-galactoside (ONPG) were purchased from Sigma Chemicals Co. (St. Louis, MO). Dansyl polymyxin B was synthesized as described previously (*21*). The lipids 1-palmitoyl-2-oleoyl-*sn*-glycero-3-phosphocholine (POPC) and 1-palmitoyl-2-oleoyl-*sn*-glycero-3-phosphoglycerol (POPG) were purchased from Northern Lipids Inc. (Vancouver, BC).

Peptide Synthesis. All peptides were synthesized by fmoc solid-phase peptide synthesis (*26*) using a model 432A peptide synthesizer (Applied Biosystems Inc., Foster City, CA) at the University of British Columbia Nucleic Acid Protein service facility.

Preparation of Liposomes. Unilamellar liposomes (0.1 μm) were prepared with POPC/POPG (7:3 w/w) using the freeze−thaw method as described previously (*27*) followed by extrusion through 0.1 μm double-stacked Nuclepore filters using an extruder device (Lipex Biomembranes, Vancouver, BC).

Tryptophan Fluorescence and Quenching Experiment. The tryptophan fluorescence measurements were taken with a luminescence spectrometer, LS50B (Perkin-Elmer). Each peptide (2 μM) was added to 1 mL of 10 mM HEPES buffer containing 0.5 mM liposomes (pH 7.5), and the peptide/liposome mixture was allowed to interact at 20 °C for 10 min. The fluorescence was excited at 280 nm, and the emission was scanned from 300 to 400 nm. The sample was stirred by a magnetic stirrer while it was being scanned. The fluorescence spectrum of each peptide with liposomes was subtracted from the spectrum of liposomes alone. A tryptophan control was used to show no interaction of this amino acid by itself with the lipid systems that were tested.

KI quenching experiments were carried out at an excitation wavelength of 280 nm. Small aliquots (10 μL) of KI were added from a 2 M stock solution to peptides in the absence or presence of liposomes. Oxidation of iodide in the stock solutions was prevented by adding 0.5 mM $Na_2S_2O_3$. The experimental data were plotted according to the Stern−

Volmer equation $F_0/F = 1 + K_{sv}[Q]$, where F_0 and F are the fluoroscence in the absence and presence of a quencher at concentration [Q], respectively, and K_{sv} is the Stern−Volmer quenching constant (*28*).

Circular Dichroism (CD) Spectrometry. CD spectra were recorded on a model J-70 spectropolarimeter (Jasco, Tokyo, Japan) connected to a Jasco data processor, using a quartz cell with a 1 mm path length. CD spectra were measured, at 25 °C, between 190 and 260 nm at a scanning speed of 10 μm/min in 10 mM sodium phosphate buffer (pH 7.2) in the presence or absence of liposomes and in 60% 2,2,2-trifluoroethanol (TFE, Acros Organics). Minor contributions of circular differential scattering by liposomes were eliminated by subtracting the CD spectrum of liposomes alone from that of the peptide in the presence of liposomes. The spectra shown are the averages of three scans. An estimate of the percentage of helical content was calculated using the K2d program (*29*).

Minimal Inhibitory Concentration (MIC) Assay. The peptide MIC for a range of microorganisms was determined by the modified broth microdilution method (*30*). The MIC was determined as the lowest peptide concentration at which growth was inhibited after overnight incubation of the plates at 37 °C. MICs were determined three times on different occasions, and the median values are shown.

Dansyl Polymyxin B Displacement Assay. The relative binding affinity of each peptide for LPS was determined using the dansyl polymyxin B displacement assay of Moore et al. (*21*). The fraction of dansyl polymyxin B remaining bound to LPS was plotted as a function of peptide concentration. Using this plot, the concentration of each peptide required to reduce the amount of bound dansyl polymyxin (10 μM) by 50% of the maximal displacement (I_{50}) was determined.

Membrane Permeabilization Assay. The outer membrane permeabilization activity of the peptide variants was determined by the 1-*N*-phenylnaphthylamine (NPN) uptake assay of Loh et al. (*31*). Briefly, an overnight culture of *E. coli* UB1005 was diluted (1:100) in MH medium and grown to an OD_{600} of 0.5−0.6. The cells were harvested, washed, and resuspended in the same volume of buffer [5 mM HEPES (pH 7.2), 5 μM carbonyl cyanide-*m*-chlorophenyl hydrazone, and 5 mM glucose]. NPN was added to a final concentration of 10 μM, and the fluorescence was measured using a Perkin-Elmer model 650-105 fluorimeter. The increase in fluorescence due to partitioning of NPN into the outer membrane was measured after the addition of various concentrations of peptides. At the highest peptide concentrations that were used, the increase in fluorescence was virtually identical for all peptides. Polymyxin B (0.64 μg/mL) was used as a positive control. The concentration of peptide leading to a 50% maximal increase in NPN uptake was recorded as P_{50}.

The cytoplasmic membrane permeability assay involved assessment in *E. coli* ML-35 of the unmasking of β-galactosidase activity for hydrolyzing the normally cytoplasmic membrane impermeable chromogenic substrate ONPG (*22*). Logarithmic phase bacteria were harvested and resuspended in 10 mM sodium phosphate (pH 7.4) containing 100 mM sodium chloride. The cell suspension was adjusted to an OD_{600} of 0.5, and ONPG was added to a final concentration of 1.5 μM. At time zero, peptide was added and the rate of production of *o*-nitrophenol over time was monitored spectrophotometrically at 420 nm. After a lag period, the rate of color increase was constant until most of the ONPG had been hydrolyzed.

Planar Lipid Bilayer Analysis. The basic methods have been reported previously (*32*). Membranes were made from 1% lipid (comprised of 0.2% diphytanoylphosphatidylglycerol and 0.8% diphytanoylphosphatidylcholine) in *n*-decane. Bilayers were painted across a 2 mm^2 hole in a Teflon divider separating two compartments containing 5−6 mL each of a bathing solution of 1 M KCl. Voltages were applied across this membrane through Calomel electrodes connected by a salt bridge, and the resultant current was boosted 10^9−10^{10}-fold by a current amplifier, monitored on a Tektronix model 7633 oscilloscope and recorded on a Rikadenki R-01 strip chart recorder.

Hemolysis of Human Red Blood Cells. Hemolytic activity of the peptides was tested against human red blood cells. Freshly collected human blood with heparin was centrifuged to remove the buffy coat, and the erythrocytes that were obtained were washed three times in saline (0.85% NaCl). Serial dilutions of the peptides in saline were prepared in round-bottomed microtiter plates using volumes of 100 μL. Red blood cells were diluted with saline to $^1/_{25}$ of a packed cell volume, and 50 μL of cells was added to each well. Plates were incubated while they were rocked at 37 °C, and the concentration of the peptide required for lysis after 4 h was taken as the minimal hemolytic concentration.

DNA Binding Assay. Plasmid pECP1 was purified using a QIAprep Spin Miniprep Kit (Qiagen, GMbH). The plasmid DNA (0.2 μg) was mixed with increasing amounts of peptides in 15 μL of TE buffer [10 mM Tris and 1 mM EDTA (pH 8.0)]. The reaction mixtures were incubated at 20 °C for 2 min before loading on a 1.2% agarose gel, and electrophoresis was performed in Tris-borate-EDTA buffer.

Synergy. The fractional inhibitory concentration (FIC) index is used to determine the synergy between antimicrobial agents (*33*). Peptide MICs against test microorganisms were determined three times on separate occasions. Two-fold serial dilutions of nalidixic acid or chloramphenicol were tested in the presence of a constant amount of peptide, equal to one-quarter of the peptide MIC. The FIC index was calculated as follows: FIC = 0.25 + MIC(antibiotic in combination)/MIC(antibiotic alone), where 0.25 is the ratio of the MIC of the peptide in combination with the MIC of the peptide by itself. An FIC index of less than 0.5 is considered to demonstrate synergy.

RESULTS

Peptide Design. In a previous study, the DNA sequence encoding the α-helical peptide $V26_p$ [a CP26 variant previously named CP2600 (*17*)] was chosen as a target for semirandom mutagenesis. Seven of the variants isolated in that study were synthesized and studied here (Figure 1). Among the affected residues, changes at positions 7, 9, 13, 14, and 17 were always conservative, i.e., K → R, L ↔ F, and A → V. Changes at positions 12, 18, and 23 were less conservative, i.e., P ↔ A and T → H/Y. The amphipathicity of the three groups of peptides, relative to the parent peptide CP26, was not altered by the additional amino acid changes, as indicated by helical wheel analysis (data not shown). On the basis of the number of proline residues, all peptides could

$CP26_p$	KWKSF**I**K**KLT**SAAK**K**V**V**TTA**KPL**ISS
$V681_n$	KWKSFLKTFKSA**V**KTVL**H**TALK**A**ISS
$V25_p$	KWKSFL**R**T**L**KS**P**AKTV**FH**TALK**A**ISS
$V26_p$	KWKSFLK**KLT**SAAK**K**VLTTALKPISS
$V1_{pp}$	KWKSFLKT**L**KSP**V**KTV**FY**TALKPISS
$V8_{pp}$	KWKSFL**R**TFKSP**VR**TV**FH**TALKPISS
$V14_{pp}$	KWKSFLKTFKSP**V**KTV**FY**TALKPISS
$V68_{pp}$	KWKSFLKTFKSPA**R**TVL**Y**TALKPISS
$V31_{pp}$	KWKSFLKTFKSPA**R**TVL**H**TALKPISS

FIGURE 1: Amino acid sequences, in the one-letter code, of the eight peptide variants and the related peptide $CP26_p$. The bold letters denote amino acid substitutions.

be grouped into nonbent, single-bend, and double-bend peptide groups (identified here by subscripts n, p, and pp, respectively), since prolines will cause a distortion or "bend" in the α-helix. The nonbent peptide $V681_n$ did not contain a proline residue and thus was predicted to form, in a lipidic environment, an undistorted α-helical structure as predicted by the molecular modeling program Insight II (Biosym Inc., San Diego, CA). The single-bend group contained peptides $V25_p$ and $V26_p$ (as well as the parent peptide $CP26_p$) with a single proline residue at the middle and C-terminal positions, respectively. The double-bend group included peptides $V1_{pp}$, $V8_{pp}$, $V14_{pp}$, $V31_{pp}$, and $V68_{pp}$, which had proline residues at both the middle and C-terminal regions.

Interaction of Peptides with Liposomes. Most studies of the interaction of cationic antimicrobial peptides with membranes have been performed using model liposomes with compositions chosen to reflect those of the bacterial cytoplasmic membrane, e.g., a mixture of the anionic lipid phosphatidylglycerol and the zwitteronic lipid phosphatidylcholine (*34*, *35*). The latter while not a bacterial lipid is structurally related to phosphatidylethanolamine, but has been preferred since it more readily forms stable bilayers. To investigate the specificity of interaction of these peptides with a membrane-mimicking environment, liposomes composed of a 7:3 mixture of POPC and POPG were used.

The fluorescence emission of the tryptophan residue present at residue 2 of each peptide provided a method for monitoring the binding of peptides to liposomes, since fluorescence of this amino acid is sensitive to environment. Upon addition to liposomes of peptides $V8_{pp}$, $V25_p$, $V681_n$, and $CP26_p$ representing the three groups, the fluorescence emission maxima of all the peptides exhibited a blue shift and a marked increase in emission intensities indicating a relocation of the peptides' tryptophan residues into a more hydrophobic environment (Figure 2A and Table 1). All tryptophan residues apparently participated in this blue shift since there was no shoulder on the emission spectrum due to unbound tryptophan. A relatively large increase in fluorescence quantum yield was observed with $CP26_p$ and $V681_n$, while a smaller increase was noted with $V25_p$ and $V8_{pp}$.

The tryptophan fluorescence intensity was decreased in a concentration-dependent manner by the addition to these peptides, in the absence of liposomes, of the water soluble quencher KI. When the quencher was added to peptide in the context of liposomes, no decrease in fluorescence intensity was observed, indicating that the tryptophan residues at position 2 of these peptides were no longer accessible to the aqueous quencher (Figure 2B).

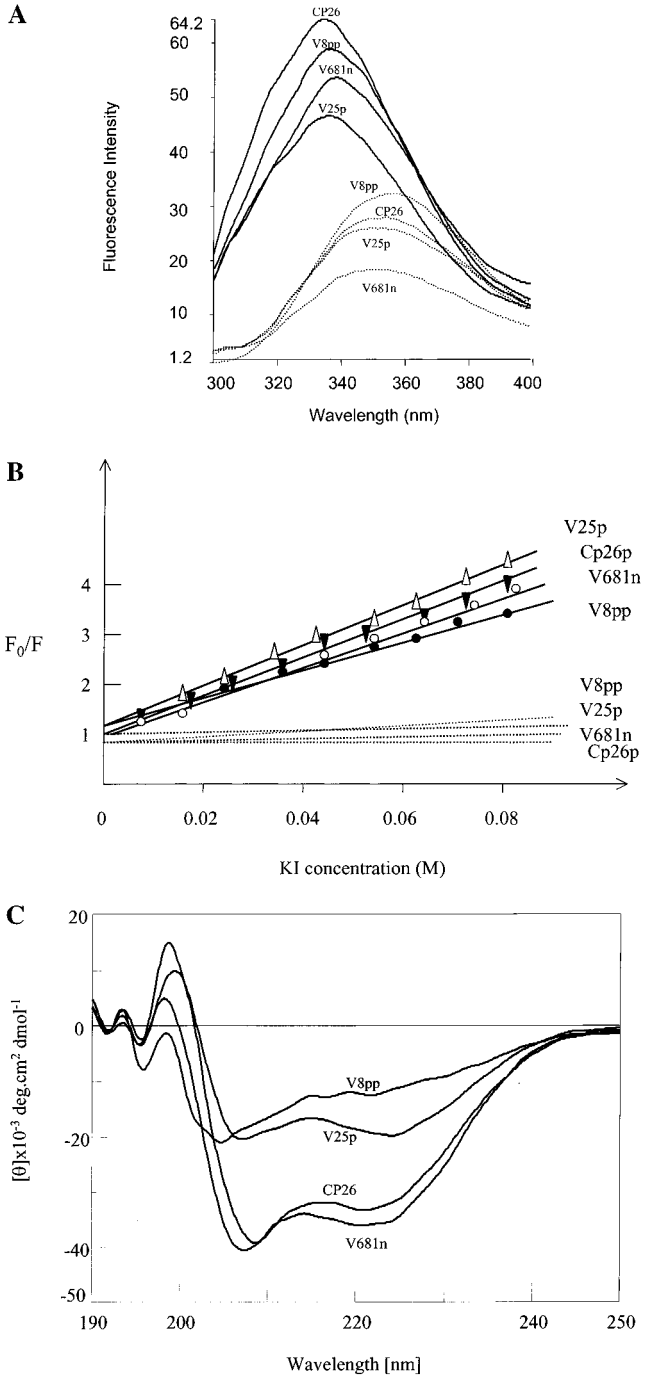

FIGURE 2: (A) Tryptophan fluorescence emission spectra of each representative peptide at 2 μM, in the presence of 100 μM of POPC/POPG liposomes (7:3). The excitation wavelength was 280 nm. Solid lines represent spectra in liposomes, while dotted lines represent spectra in 10 mM sodium HEPES buffer (pH 7.2). (B) Stern−Volmer plot of the tryptophan quenching data for quenching by an aqueous quencher KI. Dotted lines represent data for peptides in liposomes, while solid lines represent data for quenching in HEPES buffer. (C) Circular dichroism spectra of $V681_n$, $V25_p$, $Cp26_p$, and $V8_{pp}$ in POPC/POPG (7:3) liposomes. The concentration of each peptide was 50 μM added to 1 mM lipid.

CD spectra demonstrated that all three structural groups, represented by $V8_{pp}$, $V25_p$, $V681_n$, and $CP26_p$, had CD spectra typical of unstructured peptides in buffer (data not shown). However, when inserted into liposomes, at the same molar concentrations, all peptides were promoted to adopt α-helical conformations with characteristic double minima at 208 and 222 nm (Figure 2C). As expected, the estimated

Table 1: Tryptophan Fluorescence Emission Maxima of the Representative Peptides in HEPES Buffer or in the Presence of 7:3 POPC/POPG Liposomes

peptide	HEPES[a] (nm)	liposomes[b] (nm)	blue shift (nm)[c]	intensity[d]
$V681_n$	350.0	338.3	11.7	35.4
$V25_p$	350.0	336.8	13.2	20.1
$V8_{pp}$	356.4	336.3	20.1	26.5
$CP26_p$	351.6	334.5	16.5	36.3

[a] Emission maxima in HEPES buffer (±0.5 nm). [b] Emission maxima in liposome buffer (±0.5 nm). [c] Blue shift in emission maximum. [d] Relative fluorescence intensity increase.

helicities tended to decrease as the number of prolines increased with the α-helical content of these peptides, as calculated using the K2d program, being 90, 89, 61, and 31% for $V681_n$, $CP26_p$, $V25_p$, and $V8_{pp}$, respectively. These data were consistent with the concept that all of the peptides altered their configurations from a random coil to a more α-helical structure as they entered membranes. Similar CD spectra and percentages of helicity of the same peptides were also obtained using the organic solvent trifluoroethanol (data not shown).

Antimicrobial and Hemolytic Activity. The MICs of the peptide variants against a panel of microorganisms are shown in Table 2. The two single-bend peptides together with $CP26_p$ exhibited similar antimicrobial spectra and were quite active against Gram-negative bacteria and the Gram-positive bacterium *S. epidermidis*. The double-bend peptides were most active against *E. coli*, with weaker activities (MICs of 8−32 μg/mL) against other Gram-negative bacteria, although three of the peptides killed *S. epidermidis* at high concentrations (16−32 μg/mL). In contrast, the nonbent peptide $V681_n$ exhibited a very high activity against all the Gram-negative and Gram-positive bacteria that were tested with MIC values ranging from 0.5 to 4 μg/mL.

The hemolytic activity was determined using human red blood cells. The nonbent peptide $V681_n$ was highly hemolytic and lysed red blood cells at 8 μg/mL. Most of the single- and double-bend peptides were nonhemolytic, even at 128 μg/mL. However, $V1_{pp}$ and $V26_p$ lysed red blood cells at 32−64 μg/mL (Table 2).

*Synergy with Conventional Antibiotic*s. One of the known assets of antimicrobial peptides is their potential to promote the activity of conventional antibiotics in killing bacteria (*36*). However, not all peptides have this activity, and the structural basis for synergism has not been investigated. Thus, we examined in this study whether the bends introduced by proline incorporation were a factor in determining synergism. Resistant mutants of *E. coli* and *P. aeruginosa* were utilized to assess synergy. One-quarter of the MIC concentration of each peptide (Table 2) was tested for synergy with doubling dilutions of chloramphenicol or naladixic acid, and results are shown in Table 3. It is worthwhile to mention that none of the peptides killed the test microorganisms at their quarter MICs. Therefore, killing was a cooperative consequence of both the peptide and antibiotics.

All five double-bend peptides exhibited synergistic killing with both nalidixic acid and chloramphenicol against *P. aeruginosa* H374 and H744, and similar synergistic effects with nalidixic acid were also observed with *E. coli* strains KF130 and KF111. In both cases, FIC indices from 0.28 to 0.5 were achieved (where an FIC index of ≤0.5 indicates synergy; *31*). Synergy with chloramphenicol against *E. coli* strains seemed to vary among the double-bend peptides. Only $V31_{pp}$ exhibited synergy with chloramphenicol against both *E. coli* KF130 and KF111. $V14_{pp}$ and $V8_{pp}$ demonstrated synergy with chloramphenicol against each one of the two *E. coli* strains. Of the three single-bend peptides that were studied, only $V25_p$ and $CP26_p$ demonstrated synergy with both antibiotics against the *P. aeruginosa* strains and with nalidixic acid against *E. coli* KF130. Synergy was not observed with $V26_p$ or nonbent peptide $V681_n$.

LPS Binding Affinity. Gram-negative bacteria like *E. coli* have two cell envelope membranes, the outer and cytoplasmic membrane. The outer membrane is an asymmetric membrane with the bulky glycolipid, lipopoysaccharide (LPS) in its outer monolayer, and phospholipids (with a composition similar to that of the cytoplasmic membrane) in its inner monolayer. Thus, in killing *E. coli*, such peptides must interact with both membranes, and very few studies have addressed this issue, or demonstrated the preferential effect of the variation of peptide structures on one of these membranes. The initial interaction of cationic antimicrobial peptides with the bacterial cell occurs via binding of the peptides to the anionic lipid LPS, which is the sole lipid species in the outer leaflet of the outer membrane (*21*). The binding of positively charged compounds to LPS can be assessed by the displacement of a bound probe, dansyl polymyxin B, resulting in decreased fluorescence of the dansyl group (*21*). The concentration of peptide resulting in 50% maximal displacement of dansyl polymyxin (I_{50} value) can be used as an indicator of the relative binding affinity.

Table 2: Antimicrobial (MIC) and Hemolytic [Minimal Hemolytic Concentration (MHC)] Activities of Peptide Variants against Bacteria and Human Red Blood Cells (hRBC)

	MIC (μg/mL)									
	E. coli				*P. aeruginosa*					MHC
peptide	UB1005	KF130	KF111	*S. typhimurium*	K799	H374	H744	*S. epidermidis*	*S. aureus*	hRBC
$V681_n$	0.5	1	1	4	2	2	2	4	4	8
$CP26_p$	1	1	2	8	4	6	6	32	>64	>128
$V25_p$	0.5	1	1	4	16	8	8	4	32	>128
$V26_p$	1	1	1	4	8	4	4	4	32	64
$V8_{pp}$	2	4	4	8	16	16	16	16	>64	>128
$V1_{pp}$	2	2	2	16	16	16	16	32	>64	32
$V14_{pp}$	2	4	4	16	32	32	32	32	>64	>128
$V31_{pp}$	4	8	4	32	32	32	32	>64	>64	>128
$V68_{pp}$	1	2	2	16	32	16	16	>64	>64	>128

Table 3: Synergy between Peptides and Nalidixic Acid (nal) or Chloramphenicol (Cm) against *P. aeruginosa* H374 and H744 and *E. coli* KF130 and KF111

	FIC index[a]							
	H374		H744		KF130		KF111	
peptide	Nal	Cm	Nal	Cm	Nal	Cm	Nal	Cm
$V681_n$	1.25	1.25	1.25	1.25	0.75	0.75	0.75	0.75
$CP26_p$	0.375	0.5	0.5	0.75	0.5	0.75	0.5	0.5
$V25_p$	0.5	0.5	0.38	0.31	0.5	0.75	0.75	0.75
$V26_p$	1.25	1.25	1.25	0.75	0.75	0.75	0.75	0.75
$V1_{pp}$	0.28	0.312	0.26	0.26	0.375	0.75	0.5	0.75
$V8_{pp}$	0.5	0.375	0.5	0.31	0.253	0.75	0.28	0.5
$V14_{pp}$	0.28	0.312	0.26	0.26	0.375	0.5	0.375	0.75
$V31_{pp}$	0.5	0.5	0.38	0.31	0.313	0.5	0.28	0.375
$V68_{pp}$	0.375	0.312	0.31	0.28	0.375	0.75	0.5	0.75

[a] The fractional inhibitory concentration (FIC) index was used to determine synergy between antimicrobial agents. Two-fold serial dilutions of nalidixic acid or chloramphenicol were tested in the presence of a constant amount of peptide, equal to one-quarter of the peptide MIC. The FIC index was calculated as follows: FIC = 0.25 + MIC(antibiotic in combination)/MIC(antibiotic alone), where 0.25 is the ratio of the MIC of the peptide in combination to the MIC of the peptide by itself. An FIC index of <0.5 is considered to demonstrate synergy (*32*), whereas an FIC of 1 indicates additivity.

Table 4: Relative Peptide Binding to *E. coli* UB1005 and to *P. aeruginosa* H103 LPS (Assessed as the Displacement of Dansyl Polymyxin) and Peptide Permeabilization of the Outer Membrane (Assessed as NPN Uptake)

	UB1005		H103		P_{50}
peptide	I_{50} (μM)[a]	I_{max} (%)	I_{50} (μM)	I_{max} (%)[b]	(μg/mL)[c]
CP26	23	48	21	50	2.2 ± 0.2
$V681_n$	12	60	14	68	1.4 ± 0.1
$V25_p$	27	45	31	50	2.5 ± 0.1
$V26_p$	20	45	19	59	2.4 ± 0.2
$V1_{pp}$	19	50	16	60	2.1 ± 0.1
$V8_{pp}$	20	50	23	65	2.5 ± 0.3
$V14_{pp}$	24	40	16	50	3.0 ± 0.1
$V31_{pp}$	22	40	19	50	3.0 ± 0.1
$V68_{pp}$	24.	40	26	55	2.5 ± 0.1

[a] Concentration required for 50% maximal dansyl polymyxin displacement. The molecular weights of the peptides varied from 2860 to 3070. [b] Maximum displacement of dansyl polymyxin. [c] Concentration required to give 50% of the maximal increase in NPN flourescence.

As shown in Table 4, all peptides bound to both *P. aeruginosa* and *E. coli* LPS with relatively similar affinities as indicated by their I_{50} values which differed by less than 2-fold, although $V681_n$ exhibited a somewhat higher affinity for both LPS molecules. The percentages of maximum displacement of dansyl polymyxin B were similar for all peptides, and indicated that the peptides did not interact with all the dansyl polymyxin binding sites on LPS.

Membrane Permeabilization Activity. The ability of the peptide variants to permeabilize the outer membrane of *E. coli* UB1005 was determined in intact cells using the NPN uptake assay. NPN is a small hydrophobic molecule that is normally excluded by the outer membrane but exhibits increased fluorescence when it partitions into the bacterial outer membrane. Therefore, an increase in fluorescence in the presence of a peptide indicated the ability of peptide to permeabilize the bacterial outer membrane. As shown in Table 4, all the peptide variants were able to mediate NPN uptake across the outer membrane to similar extents. The P_{50} values (concentration required to cause a 50% increase in NPN florescence) differed by less than 2-fold, with $V681_n$ exhibiting a slightly lower P_{50} than the other peptides. However, there was no obvious correlation between MICs for *E. coli* which differed by up to 8-fold (Table 2) and the ability to permeabilize the outer membrane or bind to LPS (Table 4).

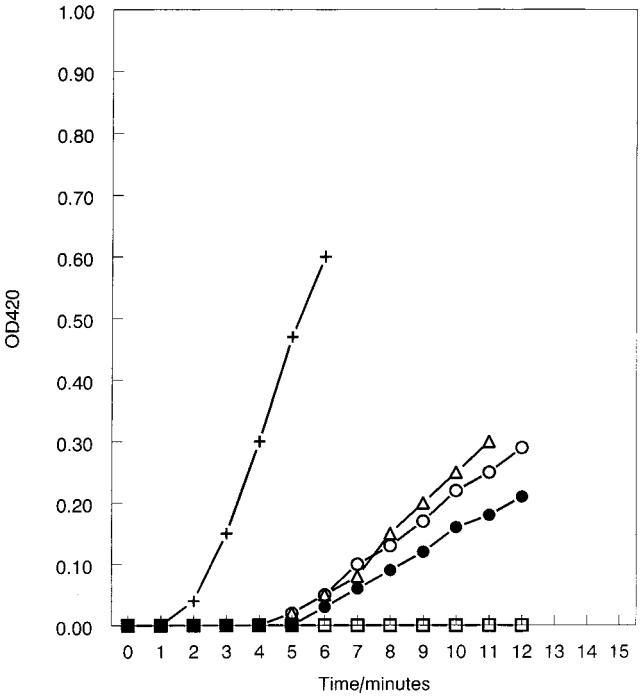

FIGURE 3: Cytoplasmic membrane permeabilization by peptides as assessed by unmasking of cytoplasmic β-galactosidase in *E. coli* ML-35. β-Galactosidase activity was assessed spectrophotometrically at 420 nm by assessing the whole cell hydrolysis of the normally impermeable, chromogenic substrate ONPG. Permeabilization was performed at a concentration of 4 μg/mL for each peptide: (+) $V681_n$, (○) $V26_p$, (△) $V25_p$, (●) CP26, and (□) $V1_{pp}$, $V8_{pp}$, $V14_{pp}$, $V31_{pp}$, and $V68_{pp}$.

The ability to permeabilize the cytoplasmic membrane of intact *E. coli* ML-35 cells was determined by assessment of the unmasking of cytoplasmic β-galactosidase. Figure 3 shows the results obtained when the peptide variants were added at a concentration of 4 μg/mL. The nonbent peptide $V681_n$ exhibited the highest degree of cytoplasmic membrane permeabilization. The permeabilization took place with only a 1−2 min lag after the addition of the peptide, and an equilibrium rate of ONPG hydrolysis (equivalent to a maximal extent of permeabilization) was achieved in 2 min. The single-bend peptides required 4−5 min of lag time, and achieved an equilibrium rate of permeabilization that was approximately 3-fold lower. The double-bend peptides were poor cytoplasmic membrane permeabilizers. At 4 μg/mL peptide, there was no cytoplasmic membrane permeabilization observed. Even at 16 μg/mL peptide (data not shown), a lag time of more than 6 min was observed and the permeabilization rate was about 20-fold slower than that observed for $V681_n$.

Channel Forming Activity. To provide a basis for understanding the results of whole cell experiments, representative peptides $V681_n$, $V25_p$, and $V8_{pp}$ were examined for their ability to influence the conductance of planar bilayer membranes. Membranes were constructed from 20% anionic lipid (diphytanoylphosphatidylglycerol, as a surrogate for *E.*

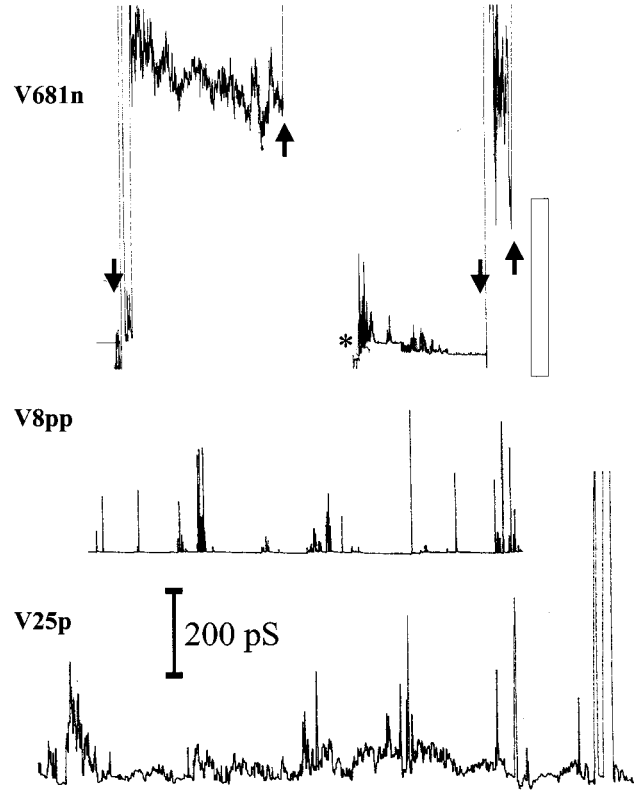

FIGURE 4: Chart recorder tracings of conductance events that occurred upon the addition of the representative peptides (1 μg/mL) to the solution (1 M KCl) bathing a planar lipid bilayer. Membranes were constructed from 1% lipid (comprising 0.2% diphytanoylphosphatidylglycerol and 0.8% diphytanoylphosphatidylcholine) in *n*-decane. Bilayers were painted across a small hole in a Teflon divider separating two compartments containing 5−6 mL each of a bathing solution of 1 M KCl. The indicated voltages were applied across this membrane through Calomel electrodes connected by a salt bridge, and the resultant current was boosted 10^9−10^{10}-fold and recorded on a strip chart recorder. Approximately 2 min of chart recordings are shown and were selected from 1−2 h of conductance experiments. The bar indicates 200 pS (1 S = 1 Ω^{-1}).

coli lipids phosphatidylglycerol and cardiolipin) and 80% zwitterionic lipid (diphytanoylphosphatidylcholine, as a surrogate for phosphatidylethanolamine). In Figure 4, some illustrative recordings of the channel forming behavior of these three peptides are presented, but the following conclusions were based on observations of hundreds of conductance events. In general, these peptides required large concentrations (approximately 1 μg/mL) to permit the observation of reasonable numbers of channels. The single-bend peptide $V25_p$ required a high voltage across the membrane (generally −180 mV) to initiate conductance across the membrane. When the applied voltage was subsequently decreased to −80 mV, conductance events were still observed but at a lower frequency. On the other hand, a positive applied voltage (e.g., 180 mV) did not initiate these conductance events, a result that seemed to be reasonable given the positive charge on this peptide. Although channel-like conductance events of variable durations (10 ms to 10 s) were observed (Figure 4) (similar to those that have been observed with other antimicrobial peptides and interpreted as multistate channels), many of the events that were observed involved very rapid conductance alterations which were quite variable in magnitude (11−194 pS). An interesting observation was that there were few situations where conductance events led to a substantial increase in overall transmembrane conductance since events tended to be rapid, and the net result was a rapid or eventual return to baseline conductance. Peptide $V25_p$ only caused rapid destabilization of the membrane at very high concentrations and a nonphysiological voltage (−280 mV). Similar types of conductance events were observed with a number of other control α-helical peptides with a single C-terminal proline, namely, $CP26_p$, CP29, CEME, and CEMA. In contrast, $V681_n$ initiated conductance events at a low transmembrane voltage (−30 mV), and higher voltages (−80 mV) resulted in very rapid membrane destabilization and breakage within a few seconds in six independent experiments (Figure 4). The observed channels were very variable in both duration (10 ms to 20 s) and magnitude (50−1250 pS).

Peptide $V8_{pp}$ exhibited very poor activity, in contrast to the other two peptides. Those conductance events observed had a very short lifetime, on the order of microseconds; therefore, it required observation of the channels on an oscilloscope to discern that the peptides were open for a finite but short time, and on the chart recording (Figure 4), the conductance events appeared as spikes of 10−400 pS conductance. The initiation voltage was, like that of $V25_p$, high, but unlike $V25_p$, reducing the voltage resulted in the complete loss of all conductance events.

DNA Binding Activity. Since there was no clear evidence that the peptides studied here worked by a membrane permeabilization mechanism, we investigated the possibility of other targets, such as DNA binding (*37*). The DNA binding activity of peptides $V681_n$, $V25_p$, and $V8_{pp}$ is shown in Figure 5. All three peptides bound to DNA within 2 min and caused retardation of DNA mobility, with minor differences. Both $V681_n$ and $V25_p$ completely inhibited DNA migration in the presence of equal amounts (by weight) of peptide (0.2 μg), while $V8_{pp}$ bound to DNA and caused relaxation of the DNA structure. However, if the DNA/peptide mixture was incubated for 10 min, even $V8_{pp}$ totally inhibited DNA mobility.

DISCUSSION

Proline is an amino acid that creates a rigid bend in the peptide backbone since the carboxyl and amino groups of this backbone are covalently bound. Thus, proline is generally accepted as a helix breaker. In this paper, we studied nine peptides either lacking proline or including one or two proline residues, in addition to two to five conservative and nonconservative amino acid substitutions, that had been made via semirandom mutagenesis of $V26_p$ (*18*). $V26_p$ and the related peptide CP26 have a single proline residue in their C-terminal regions. This general feature (a single proline residue and/or two glycines) is quite common among the natural α-helical peptides.

All of the peptides we studied were relatively unstructured in free solution, and had some degree of α-helicity when the peptides inserted into liposomes. Although the percentage of helicity seemed to be lower for the double-bend peptide, $V8_{pp}$, and intermediate for the single-bend peptide, $V25_p$, a result consistent with the observations of other researchers working with proline substitution variants of antimicrobial peptides (*13*−*16*), the CD spectra in liposomes still indicated preferentially α-helical structures. For this limited subset,

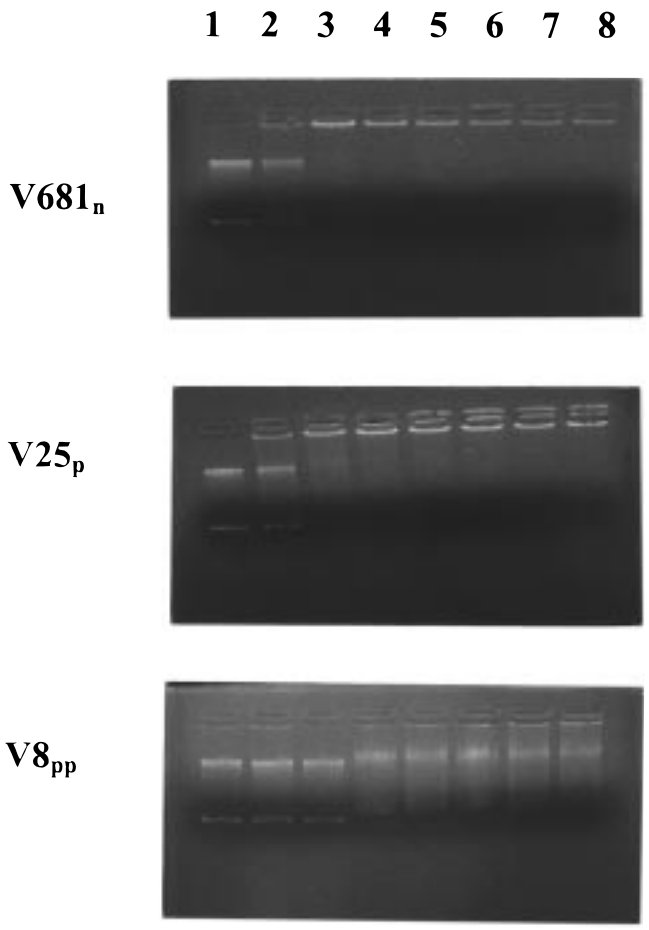

FIGURE 5: Interaction of peptides with plasmid DNA. Two hundred nanograms of plasmid DNA was used: lane 1, plasmid DNA alone; lane 2, 0.1 μg of peptide; lane 3, 0.2 μg of peptide; lane 4, 0.3 μg of peptide; lane 5, 0.4 μg of peptide; lane 6, 0.5 μg of peptide; lane 7, 0.6 μg of peptide; and lane 8, 0.7 μg of peptide. DNA and the peptides were co-incubated for 2 min at 23 °C before loading onto a 1.2% agarose gel and electrophoresis.

there was no obvious trend in activity against bacteria that accompanied the different α-helicities. For example, $CP26_p$ (89% helicity) had activities similar to those of $V25_p$ (61% helicity) against *E. coli*, whereas $V25_p$ and $V8_{pp}$ (35% helicity) were most similar in activity against *Pseudomonas*, and all three peptides had similar anti-*Salmonella* activity (Table 2). We are cognizant that the programs for resolving CD spectra in terms of estimated α-helicity are based on CD spectral studies of proteins that have been crystallized and thus may have limited relevance to the interpretation of the spectra of peptides.

Regardless of the structural variations, at the concentrations that were tested, all of the peptides tended to bind to liposomes as shown by tryptophan fluorescence spectroscopy. In general, tryptophans buried within a hydrophobic milieu exhibit a higher quantum yield of fluorescence, and the position of their emission maximum is blue-shifted when compared with those of the tryptophans that are accessible to solvent (Figure 2A). Although the blue shift of $V681_n$ in liposomes seemed to be smaller than that for the other peptides, it is worth noting that $V681_n$ tended to form a small degree of α-helical structure even in buffer (data not shown). The blue shifts and the increase in intensity of the emission maxima when the peptides inserted into liposomes suggested that the single tryptophan residue of all peptides was inserted into the hydrophobic lipid phase (or interface) of the bilayer. This was more evident with a quenching assay showing that the tryptophan residue of each peptide was no longer accessible to the quencher KI. However, both of the blue shifts and the intensity maxima varied from peptide to peptide (Table 1, columns 4 and 5), and we postulate that this could be due to different configurations and orientations of the peptides in the membrane bilayer. This could then influence the ability of peptides to aggregate into channel-like conducting structures, as clearly observed in in vivo cytoplasmic membrane permeabilization and the planar lipid bilayer experiments (Figures 3 and 4). The double-bend peptides were unable to permeabilize the cytoplasmic membrane to ONPG, at concentrations around or above the MIC (4 μg/mL) (Figure 3), and $V8_{pp}$ formed only conductance spikes at high voltages. The single-bend peptides demonstrated a weak ability to permeabilize the cytoplasmic membrane of *E. coli*, and $V25_p$ and $CP26_p$ formed channels with a high activation voltage (−180 mV) and variable magnitude and duration. Such conductance events have been observed with other antimicrobial peptides, and proposed to be due to the formation of multistate channels (*38*) or a transient translocation of peptide across membrane by a micellar aggregate mechanism (*39*). $V681_n$, which had the broadest activity spectrum, including hemolytic activity, demonstrated the greatest ability to disrupt the cytoplasmic membrane. It also formed multistate channels, some of which had quite long durations (Figure 4). However, its most obvious differentiating features were its ability to initiate conductance events at low voltages (−30 and −180 mV for the single- and double-bend peptides, respectively) and its ability to destabilize the membrane (at −80 mV for the single- and double-bend peptides which only caused membrane breakdown at extremely high, nonphysiological voltages of −280 mV). Since bacterial cytoplasmic membranes carry large electrical potential gradients (−140 mV) in contrast to most eukaryotic cells (−15 mV or so), we suggest that the low "trigger" voltage for causing conductance and the ability to promote membrane disruption explains why only $V681_n$ is strongly hemolytic. On the other hand, neither the single- nor double-bend peptides seem to cause bacterial cytoplasmic membrane breakdown at physiological transmembrane potential electrical gradients (the single-bend peptides were weak cytoplasmic membrane-permeabilizing agents even at a level 4−8 times greater than the MIC). Since both groups of peptides kill Gram-negative bacteria, we feel that this is further evidence that the mechanism of killing does not necessarily involve the action of peptides on membranes, and definitely does not involve membrane lysis.

Although we have not elucidated the mechanism and the mode of action of the proline-containing peptides, we feel that they must target other cellular components to confer microbicidal activity. Recent studies have shown that both membrane lytic and nonlytic cationic peptides are able to bind DNA and inhibit DNA migration, as shown by gel retardation experiments (*37*). In agreement with this, we showed here that the representative peptides were able to interact with DNA. Thus, polyanionic DNA could be one of the targets for cationic peptides. Alternatively, due to their amphipathic nature, cationic peptides have the potential to interact with both anionic and hydrophobic materials, sug-

gesting that there are other mechanisms of action, including stimulation of autolytic enzymes (*40*), and interference with bacterial DNA and/or protein synthesis (*41*, *42*). In contrast to the proline-containing peptides, it is possible that $V681_n$ may kill bacteria by membrane lysis.

Our study confirms observations that a membrane-lytic α-helical peptide can be modified into a nonmembrane lytic peptide by introduction of proline residues. This is consistent with observations made with a 16-residue model cationic peptide (*14*) and a noncationic peptide alamethicin (*43*), where it was found that removing a proline in the central position of the molecule decreased hemolytic activity (in the former case without decreasing antibacterial activity). Conversely, removal of proline-7 from pardaxin made the molecule more hemolytic (*15*).

The ability of the peptides to synergize with conventional antibiotics was inversely correlated with their antimicrobial activities and ability to cause permeabilizing events in bilayers. The interaction of antimicrobial peptides with the outer membrane has been proposed to be responsible in part for this property of synergy with antibiotics. To reach the cytoplasmic membrane, a cationic peptide must overcome the outer membrane barrier. The initial interaction of cationic peptides with the bacterial outer membrane involves electrostatic binding to the negatively charged, divalent cation-binding sites on the surface glycolipid lipopolysaccharide (LPS), and competitive displacement of these cations (*2*). Such an interaction causes a distortion of outer membrane structure and a consequent permeabilization of the membrane to probe molecules, and to the peptide itself. Our data indicate that all three groups of peptides are able to bind to LPS and to permeabilize the outer membrane to similar extents, suggesting that they should have a similar ability to promote the passage of other molecules such as chloramphenicol and nalidixic acid. We propose that the nonbent peptide causes cell death at the same concentration at which it permeabilizes the outer membrane. Thus, it cannot exhibit synergy since it would promote the uptake of other antibiotics only at the killing concentration. Conversely, the double-bend peptides would permeabilize the outer membrane at concentrations lower than those required to result in a lethal event, such that uptake of chloramphenicol and nalidixic acid would be promoted and synergy (i.e., enhanced killing by these conventional antibiotics) would occur. This means that technically speaking it should be possible to make a peptide which has no ability to kill cells but can still exhibit synergy with conventional antibiotics.

In conclusion, our data strongly indicated that (1) replacement of a single proline in an α-helical peptide may turn an antimicrobial peptide into a toxin; (2) peptide sequence changes can influence insertion into liposomes, bacterial inner membrane permeability, and hemolysis, independently; (3) one can create a novel class of therapeutic agents devoid of antimicrobial activity, but able to exhibit synergy with conventional antibiotics; and (4) cytoplasmic membrane may not be the target for antimicrobial cationic peptides.

REFERENCES

Boman, H. G. (1995) *Annu. Rev. Immunol. 13*, 61−92.

Hancock, R. E. W., and Lehrer, R. I. (1998) *Trends Biotechnol. 16*, 82−88.

Lehrer, R. I., and Ganz, T. (1996) *Ann. N.Y. Acad. Sci. 797*, 228−239.

Hancock, R. E. W. (1997) *Lancet 349*, 418−422.

Lohner, K., Latal, A., Lehrer, R. I., and Ganz, T. (1997) *Biochemistry 36*, 1525−1531.

Kagan, B. L., Selsted, M. E., Ganz, T., and Leher, R. I. (1990) *Proc. Natl. Acad. Sci. U.S.A. 87*, 210−214.

Ludtke, S., He, K., Heller, W. T., Harroun, T. A., Yang, L., and Huang, H. W. (1996) *Biochemistry 35*, 13723−13728.

Segrest, J. P., de-Loof, H., Dohlman, J. G., Brouillette, C. G., and Anantharamaiah, G. M. (1990) *Proteins 8*, 103−117.

Saberwal, G., and Nagaraji, R. (1994) *Biochim. Biophys. Acta 1197*, 109−131.

Wieprecht, T., Dathe, M., Epand, R. M., Beyermann, M., Krause, E., Maloy, W. L., MacDonald, D. L., and Bienert, M. (1997) *Biochemistry 36*, 12869−12880.

Dathe, M., Schümann, M., Wieprecht, T., Winkler, A., Beyermann, M., Krause, E., Matsuzaki, K., Murase, O., and Bienert, M. (1996) *Biochemistry 35*, 12612−12622.

Dathe, M., Wieprecht, T., Nikolenko, H., Handel, L., Maloy, W. L., MacDonald, D. L., Beyermann, M., and Bienert, M. (1997) *FEBS Lett. 403*, 208−212.

Gazit, E., Boman, A., Boman, H. G., and Shai, Y. (1995) *Biochemistry 34*, 11479−11488.

Thennarasu, S., and Nagaraj, R. (1995) *Int. J. Pept. Protein Res. 46*, 480−486.

Thennarasu, S., and Nagaraj, R. (1997) *Biopolymers 41*, 635−645.

Andreu, D., Merrifield, R. B., Steiner, H., and Boman, H. G. (1985) *Biochemistry 24*, 1683−1688.

Zhang, L., Falla, T., Wu, M., Fidai, S., Burian, J., Kay, W., and Hancock, R. E. W. (1998) *Biochem. Biophys. Res. Commun. 247*, 674−680.

Richmond, M. G., Clarke, D. C., and Wotton, S. (1976) *Antimicrob. Agents Chemother. 10*, 215−218.

Fields, P. I., Grosman, E. A., and Heffron, F. (1989) *Science 243*, 1059−1062.

Angus, B. L., Carey, A. M., Caron, D. A., Kropinski, A. M. B., and Hancock, R. E. W. (1982) *Antimicrob. Agents Chemother. 21*, 299−309.

Moore, R. A., Bates, N. C., and Hancock, R. E. W. (1986) *Antimicrob. Agents Chemother. 29*, 496−500.

Lehrer, R. I., Barton, A., Daher, K. A., Harwig, S. S. L., Ganz, T., and Selsted, M. E. (1989) *J. Clin. Invest. 84*, 553−561.

Hooper, D. C., Wolfson, J. S., Ng, E. Y., and Swartz, M. N. (1987) *Am. J. Med. 82* (Suppl. 4A), 12−20.

Masuda, N., and Ohya, S. (1992) *Antimicrob. Agents Chemother. 36*, 1847−1851.

Poole, K., Krebes, K., McNally, C., and Neshat, S. (1993) *J. Bacteriol. 175*, 7363−7372.

Merrifield, R. B. (1986) *Science 232*, 341−347.

Mayer, L. D., Hope, M. J., Cullis, P. R., and Janoff, A. S. (1985) *Biochim. Biophys. Acta 817*, 193−196.

Eftink, M. R., and Ghiron, C. A. (1976) *J. Phys. Chem. 80*, 486−493.

Andrade, M. A., Chacón, P., Merelo, J. J., and Morán, F. (1993) *Protein Eng. 6*, 383−390.

Wu, M., and Hancock, R. E. W. (1999) *J. Biol. Chem. 274*, 29−35.

Loh, B., Grant, C., and Hancock, R. E. W. (1984) *Antimicrob. Agents Chemother. 26*, 546−551.

Benz, R., and Hancock, R. E. W. (1981) *Biochim. Biophys. Acta 646*, 298−308.

Amsterdam, D. (1991) in *Antibiotics in laboratory medicine* (Lorian, V., Ed.) 3rd ed., pp 72−82, Williams and Wilkins, Baltimore, MD.

Ghosh, A. K., Rukmini, R., and Chattopadhyay, A. (1997) *Biochemistry 36*, 14291−14305.

Breukink, E., van Kraaij, C., van Dalen, A., Demel, R. A., Siezen, R. J., de Kruijff, B., and Kuipers, O. P. (1998) *Biochemistry 37*, 8153−8164.

Scott, M., Yan, H., and Hancock, R. E. W. (1999) *Infect. Immun. 67*, 2005−2009.

Park, C. B., Kim, H. S., and Kim, S. C. (1998) *Biochem. Biophys. Res. Commun. 244*, 253−257.

Kordel, M., Benz, R., and Sahl, H. G. (1988) *J. Bacteriol. 170*, 84−88.

Hancock, R. E. W., and Chapple, D. (1999) *Antimicrob. Agents Chemother*. (in press).

Chitnis, S. N., Prasad, K. S. N., and Bhargava, P. M. (1990) *J. Gen. Microbiol. 136*, 463−469.

Boman, H. G., Agerbath, B., and Boman, A. (1993) *Infect. Immun. 61*, 2978−2984.

Subbalakshmi, C., and Sitaram, N. (1998) *FEMS Microbiol. Lett. 160*, 91−96.

Dathe, M., Kaduk, C., Tachikawa, E., Melzig, M. F., Wenschuh, H., and Bienert, M. (1998) *Biochim. Biophys. Acta 1370*, 175−183.

BI9904104